LETTERS
PUBLISHED ONLINE: 27 JULY 2014 | DOI: 10.1038/NCLIMATE2323

nature climate change

The emerging anthropogenic signal in land–atmosphere carbon-cycle coupling

Danica Lombardozzi*, Gordon B. Bonan and Douglas W. Nychka

Earth system models simulate prominent terrestrial carbon-cycle responses to anthropogenically forced changes in climate and atmospheric composition over the twenty-first century[1–4]. The rate and magnitude of the forced climate change is routinely evaluated relative to unforced, or natural, variability using a multi-member ensemble of simulations[5–8]. However, Earth system model carbon-cycle analyses do not account for unforced variability[1–4,9]. To investigate unforced terrestrial carbon-cycle variability, we analyse ensembles from the Coupled Model Intercomparison Project (CMIP5), focusing on the Community Climate System Model (CCSM4). The unforced variability of CCSM4 is comparable to that observed at the Harvard Forest eddy covariance flux tower site. Over the twenty-first century, unforced variability in land–atmosphere CO_2 flux is larger than the forced response at decadal timescales in many areas of the world, precluding detection of the forced carbon-cycle change. Only after several decades does the forced carbon signal consistently emerge in CCSM4 and other models for the business-as-usual radiative forcing scenario (RCP8.5). Grid-cell variability in time of emergence is large, but decreases at regional scales. To attribute changes in the terrestrial carbon cycle to anthropogenic forcings, monitoring networks and model projections must consider the timescale at which the forced biogeochemical response emerges from the natural variability.

The carbon cycle influences climate through the carbon-concentration response, which is the gain in carbon storage with higher atmospheric CO_2 concentration, and the carbon–climate response, which is the loss in carbon storage with climate change[1,3]. Previous carbon-cycle analyses have emphasized these responses at multi-decadal to centennial timescales and their multi-model uncertainty[1–4,9]. Although these analyses quantify long-term carbon-cycle–climate feedbacks, they do not identify decadal-scale unforced variability in the carbon cycle.

Earth's climate has unforced variability internal to the climate system, generally termed natural variability in the climate science literature, which is an important factor in detecting the change in climate from anthropogenic forcings. Natural variability manifests as interannual-to-decadal climate variability, seen in observations and an individual model realization, as well as ensemble variability within a model[5–8]. To confidently detect and attribute changes in temperature to increases in greenhouse gases, for example, one can determine the time when the signal of the forced temperature change becomes large relative to its natural variability[8,10,11], also known as the time of emergence. Despite its importance in determining when a climate signal can be detected, however, natural variability is not considered in analyses of the twenty-first century carbon cycle[1–4]. In this work, we determine when changes in the forced carbon signal can be detected by incorporating analyses of natural variability in Earth system models (ESMs), quantified using a multi-member ensemble of simulations.

We evaluated the magnitude, timing, and spatial dependence of variability in terrestrial carbon pools (total ecosystem carbon, the sum of vegetation and soil carbon) and net land–atmosphere CO_2 fluxes (net ecosystem exchange, NEE) through the twenty-first century to determine when future changes in the carbon cycle were detectable, defined as the time when the forced signal emerged from the noise of natural variability. Analyses were completed using a six-member ensemble of the Community Climate System Model version 4.0 (CCSM4) simulations for Representative Concentration Pathway 8.5 (RCP8.5; ref. 7), which has a radiative forcing of 8.5 W m^{-2} at year 2100, with a CO_2 concentration of about 936 ppm. The six-member CCSM4 ensemble has a 3.53 °C global surface temperature warming averaged for the last 20 years of the twenty-first century compared to the 1986–2005 reference period. We additionally analysed flux tower data and a seven-member ensemble of the CCSM4 historical twentieth century simulations from 1992 through 2004 (the time period when flux data are available) for Harvard Forest to compare observed variability to model variability. We also analysed two other CMIP5 models; these models included a terrestrial carbon cycle in their RCP8.5 simulations and four or more ensemble members.

The CCSM4 has a prognostic terrestrial carbon cycle driven by the simulated climate change arising from the radiative forcings, CO_2 concentration, nitrogen deposition, and land-use and land-cover change. The land surface in the CCSM4 is a sink for carbon in the absence of anthropogenic land-use and land-cover change, but release of carbon from these activities results in a small net source of carbon over the twenty-first century[12], whereas other ESMs project a net carbon sink[2,4]. This occurs because the model has low carbon-concentration uptake compared with other ESMs (ref. 3). Under RCP8.5, cumulative ecosystem carbon projections among CMIP5 models at the end of the twenty-first century, relative to 2005, range from approximately −184 to 500 Pg C, with CCSM4 projecting a change of −69 Pg C (ref. 2). The model ranks 12th for soil carbon and 13th for vegetation carbon skill among the 18 CMIP5 models[9].

Natural variability was seen in both observational flux tower measurements and in CCSM4 simulations. Annual NEE at Harvard Forest in Massachusetts over the period 1992–2004 averaged −245 g C m^{-2} yr^{-1} (negative NEE indicates a carbon sink), and the sink increased annually at a rate of −15 g C m^{-2} yr^{-2} ($r^2 = 0.34$; ref. 13). The detrended annual anomaly ranged from −180 to 145 g C m^{-2} yr^{-1} (Fig. 1a; mean absolute value of the anomalies was 62 g C m^{-2} yr^{-1}). The seven-member CCSM4 twentieth-century ensemble simulated a modest sink for the same period at the corresponding model grid cell (Fig. 1b; 13-year ensemble mean, −19 g C m^{-2} yr^{-1}). In any given year the forest

National Center for Atmospheric Research, P.O. Box 3000, Boulder, Colorado 80307, USA. *e-mail: dll@ucar.edu

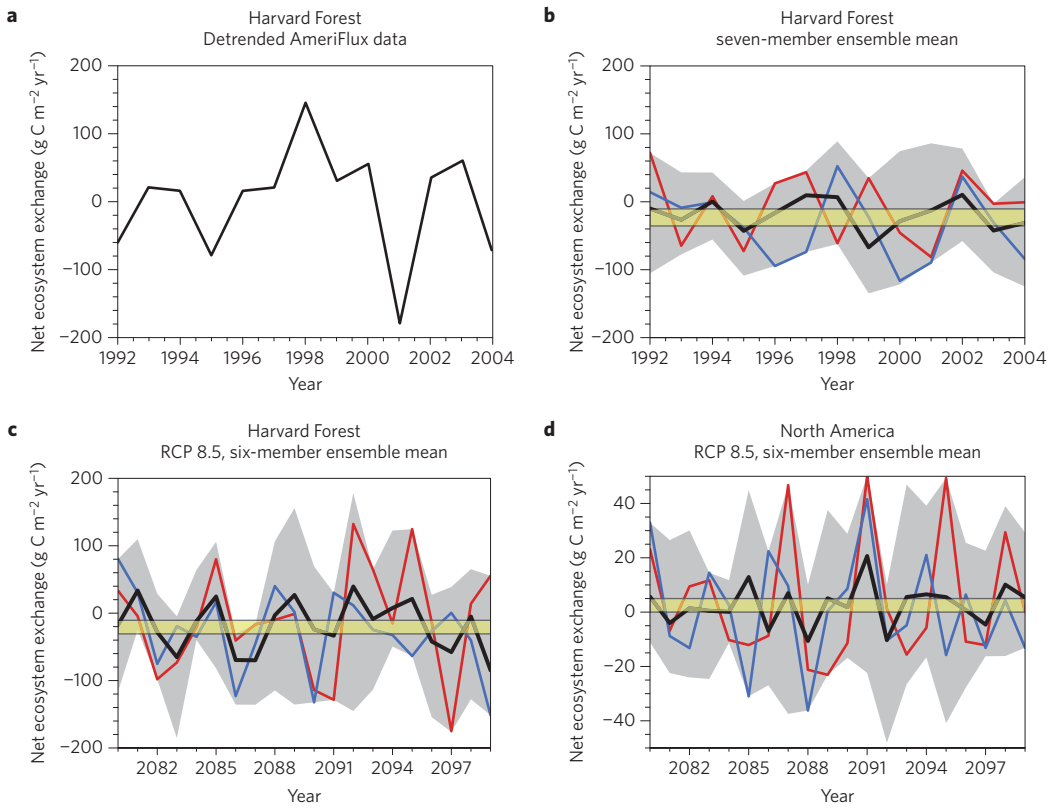

Figure 1 | Natural variability in net ecosystem exchange (NEE) from observations and CCSM4. a, Detrended interannual variability at Harvard Forest (42.538° N, 72.171° W) for 1992–2004 (ref. 13). Shown are anomalies from the long-term trend. **b**, Simulated annual NEE for a seven-member CCSM4 ensemble for 1992–2004. Shown are the ensemble mean (thick black line), and the two ensemble members with the largest (red line) and smallest (blue line) 13-year (inclusive) mean NEE for the model grid cell corresponding to Harvard Forest. The shading denotes the ensemble range for each year. The area highlighted in yellow shows the ensemble range of the 13-year means for individual ensemble members. **c**, As in **b** for the grid cell corresponding to Harvard Forest, but for a six-member CCSM4 ensemble for 2080–2099. The area highlighted in yellow shows the ensemble range of the 20-year means for individual ensemble members. **d**, As in **c**, but averaged for North America.

was either a source or sink of carbon (37% and 63% of the time, respectively, across ensemble members). Despite the larger spatial scale of a model grid cell, the interannual variability within each individual ensemble member was similar to the Harvard Forest flux tower, on the order of $\pm 100\,\mathrm{g\,C\,m^{-2}\,yr^{-1}}$. The ensemble range for any particular year was similar in magnitude, and ensemble variability over the period 2080–2099 was also comparable (Fig. 1c). Other eddy covariance flux tower sites show ranges of variability similar to the measured and simulated Harvard Forest. A synthesis of flux measurements found that interannual variability in NEE was $86\,\mathrm{g\,C\,m^{-2}\,yr^{-1}}$ in North American deciduous broadleaf forests and $44\,\mathrm{g\,C\,m^{-2}\,yr^{-1}}$ in evergreen needle-leaf forests[14]. When analyses were scaled to larger regions, ensemble variability decreased. For example, ensemble variability averaged for North America was $\pm 40\,\mathrm{g\,C\,m^{-2}\,yr^{-1}}$ at the end of the twenty-first century (Fig. 1d), with each of the ensemble members providing an equally likely realization of the twenty-first century carbon–climate system.

The time of emergence is defined as the year at which the forced climate change signal (S, for example, change in annual temperature) exceeds the noise (N, for example, standard deviation of annual temperature) by a particular threshold (for example, $S/N > 1$ or > 2; ref. 10). The time of emergence for temperature can range from a few decades in the mid-latitudes to several decades in regions with high natural variability[10]. The CCSM4 terrestrial carbon cycle has a similar timescale at which the forced signal emerges from the natural variability (Fig. 2a–d; illustrated for individual grid cells in Supplementary Fig. 1). At the end of the twenty-first century, the CCSM4 forced response (that is, the change in the mean of the multi-member ensemble) was much larger than the natural variability (that is, the standard deviation of the ensemble members) in all regions (Fig. 2d, $|S/N| > 4$). At this 90-year timescale, a single ensemble member reliably simulates the accumulated change in ecosystem carbon.

In contrast, the forced carbon signal is largely not detectable at 10 years in CCSM4 (Fig. 2a, $|S/N| < 2$ in most regions), and only detectable in specific regions at 25 years (Fig. 2b). At these decadal timescales, attributing changes in terrestrial carbon to a forced response is not reliable, and analysing a single ensemble member can be misleading. Only after 50 years does the forced carbon signal significantly exceed the natural variability in broad continental regions (Fig. 2c, $|S/N| > 2$). Unlike temperature[15], the carbon-cycle signal in low latitudes does not emerge early, and in parts of the Amazon the signal changes from carbon gain at 25 years to carbon loss at 90 years. However, there is lower confidence in the simulated carbon cycle at low latitudes as a result of the CCSM4 carbon and nitrogen interactions[16].

Analysis of other CMIP5 carbon-cycle simulations demonstrated similar timescales in the emergence of the forced response (Fig. 2e–l). The forced carbon signal emerges from the noise in most locations after 50–90 years in the Hadley Center Global Environmental Model version 2 with the Earth System configuration (HadGEM2-ES; Fig. 2g,h) and the Second Generation Canadian Earth System Model (CanESM2; Fig. 2k,l), but the signal is not detectable at 10 years in CanESM2 and is only detectable in the Arctic at 10 years in HadGEM2-ES (Fig. 2i,e). The signal is detectable in some regions within 25 years in both models (Fig. 2f,j),

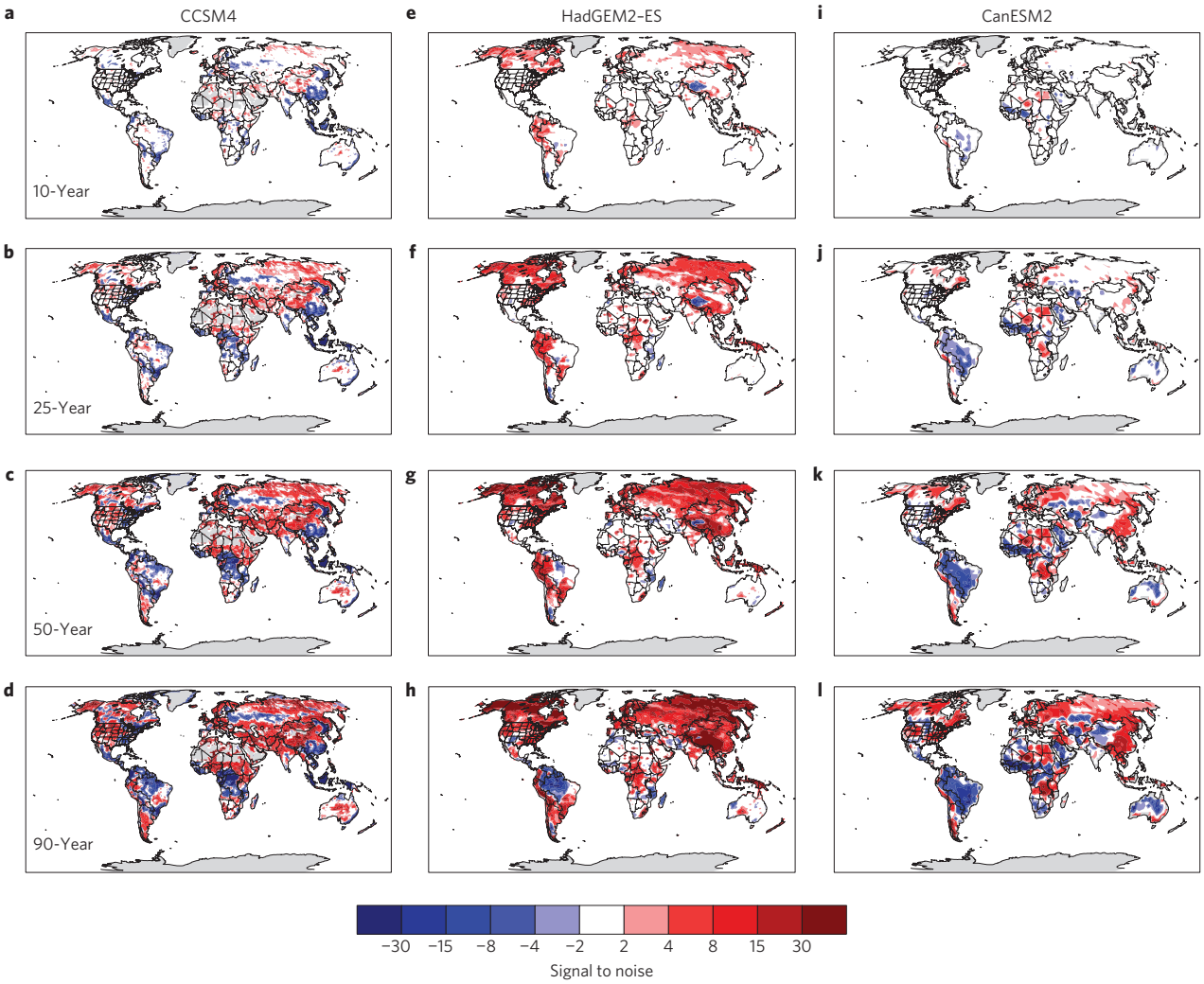

Figure 2 | Signal-to-noise ratio maps for ecosystem carbon in three ESMs. Signal (S) to noise (N) is defined as the forced (ensemble mean) change in ecosystem carbon divided by the standard deviation of the individual ensemble members. Only significant regions, defined as $|S/N| > 2$, are shown (red, carbon gain; blue, carbon loss). Maps for CCSM4 ($n = 6$) are shown in **a**–**d**, for HadGEM2-ES ($n = 4$) in **e**–**h**, and for CanESM2 ($n = 5$) in **i**–**l**. **a**,**e**,**i**, 10-year response. **b**,**f**,**j**, 25-year response. **c**,**g**,**k**, 50-year response. **d**,**h**,**l**, 90-year response.

but the regions of emergence vary depending on the model. By the end of the twenty-first century, a positive signal in the Arctic and a negative signal in the Amazon emerge in all three models, although the direction of signal emergence varies among models in other regions, such as Central Asia and eastern North America. There are known differences in carbon cycling among the models[2,9] that result in differences in the timing, magnitude and direction of signal emergence.

Natural climate variability is particularly large on small spatial scales (Fig. 2), but is often different when considered over regional or continental scales (illustrated for CCSM4 in Table 1). Climate change detection and attribution has a strong regional dependence[8,10,11,15], and our results suggest similar regional limits to detectability because the geography of natural climate variability combines with the regional nature of the forcings (that is, climate change, anthropogenic land-use and land-cover change, nitrogen deposition and CO_2 fertilization) to impart geographic variation in the time at which the carbon response emerges (Fig. 2). The forced change in carbon storage in CCSM4, for example, emerges across much of Southeast Asia within 25 years (Fig. 2b), but the regionally averaged time of emergence decreases to 10 years (Table 1). In parts of Europe, the CCSM4 forced carbon-cycle signal emerges within 25 years (Fig. 2b), but the regionally averaged signal does not emerge within 90 years (Table 1), because locations of carbon gain are averaged with locations of carbon loss to produce a small net carbon change. This highlights that it is essential in monitoring networks to carefully determine the spatial and temporal scales necessary to robustly monitor, detect and attribute changes in ecosystem carbon fluxes to forcings.

Temperature, precipitation and other meteorological factors drive variability in NEE in flux tower observations[13,17–19] and in the models. Although regional differences in temperature and precipitation variability produced geographic uncertainty in twenty-first century climate, the comparable uncertainty in the terrestrial carbon cycle was not always geographically the same, illustrated for North America in Fig. 3 using results from CCSM4. Ensemble variability in summer NEE (when metabolic activity was greatest) was highest in the central United States and parts of Canada (Fig. 3a), and these regions also had large ensemble variability in summer temperature and precipitation (Fig. 3b,c). However, regions of high climate variability did not necessarily correspond to regions of high NEE variability. For example, northeast Canada and southeast Alaska had high precipitation variability but low NEE variability, and regions of Canada had high temperature variability but low NEE variability. Similar to observations[20,21], carbon gain via net primary productivity was more strongly

Table 1 | Emergence of ecosystem carbon signal in CCSM4.

Region Name	Northwest Bound	Southeast Bound	Years to Emergence
Canadian Arctic	90° N, 120° W	66.5° N, 60° W	34
Northwest Canada	66.5° N, 125° W	55° N, 125° W	62
Central Canada	62° N, 100° W	50° N, 80° W	36
Eastern Canada	60° N, 80° W	50° N, 55° W	>90
Alaska	66.5° N, 170° W	59° N, 140° W	25
Western US	50° N, 130° W	30° N, 105° W	34
Central US	50° N, 105° W	30° N, 90° W	71
Eastern US	50° N, 90° W	30° N, 70° W	37
Northern Europe	70° N, 5° E	60° N, 45° E	36
Europe	60° N, 10° W	45° N, 30° E	>90
Western Siberia	66.5° N, 60° E	55° N, 90° E	>90
Eastern Siberia	66.5° N, 90° E	50° N, 140° E	18
Southeast Asia	23.5° N, 90° E	10° N, 120° E	10
Central Asia	50° N, 55° E	35° N, 70° E	16
Central America	16° N, 95° W	5° N, 75° W	22
Amazonia	0° N, 70° W	10° S, 50° W	46
Central Africa	5° N, 10° E	5° S, 30° E	16
Indonesia	10° N, 90° E	10° S, 150° E	6

The number of years after 2011 at which the forced (ensemble mean) signal (S) in ecosystem carbon averaged for predefined regions significantly emerges from the noise (N), or standard deviation of the individual ensemble members, for the first time in that region. Emergence is considered significant at $|S/N| > 2$.

correlated to temperature and precipitation than carbon lost during heterotrophic respiration (Supplementary Fig. 2).

Continuous and long-term measurements of net CO_2 exchange between terrestrial ecosystems and the atmosphere provide a tool to monitor ecosystem response to environmental change. Multi-year to decadal eddy covariance flux studies in forests exhibit trends in carbon storage, which arise from many factors[13,19,22–24]. Our analyses suggest that decadal trends cannot be attributed to anthropogenic forcings. This is evident in the time of emergence (>10 years, Fig. 2), but also in large ensemble variability in annual NEE for both an individual grid cell (Fig. 1c) and North America (Fig. 1d). This conclusion highlights the necessity for multi-decadal ecological monitoring networks to reliably detect forced carbon-cycle changes.

Earth system models simulate a decline in the capacity of terrestrial ecosystems to store anthropogenic CO_2 emissions over the twenty-first century[1–4], and observational analyses have attempted to detect such a trend (reviewed by ref. 25). Our work demonstrates that detection of sustained changes in land–atmosphere carbon-cycle coupling occurs only on multi-decadal or longer timescales in three different ESMs. Given the large uncertainty in carbon-cycle projections[2,4,9], our results suggest that ESMs should quantify when the forced carbon-cycle signal emerges from the natural variability. This would allow further differentiation among ESMs in their terrestrial carbon-cycle projections and may, once a detectable signal emerges, provide a constraint on the models. Further research to attribute these changes to anthropogenic forcings, and to predict the near-term decadal carbon cycle, is necessary to determine how the terrestrial carbon cycle is responding to Earth system changes, and the effectiveness of carbon-cycle management to mitigate these changes. The scientific methods of climate change detection and attribution[26], and similarly decadal climate prediction[27], emphasize the importance of natural climate variability. Our work highlights the need for these methods to be likewise applied to carbon-cycle science in future multi-model comparisons to enable detection, attribution and prediction of Earth system change, not just climate change.

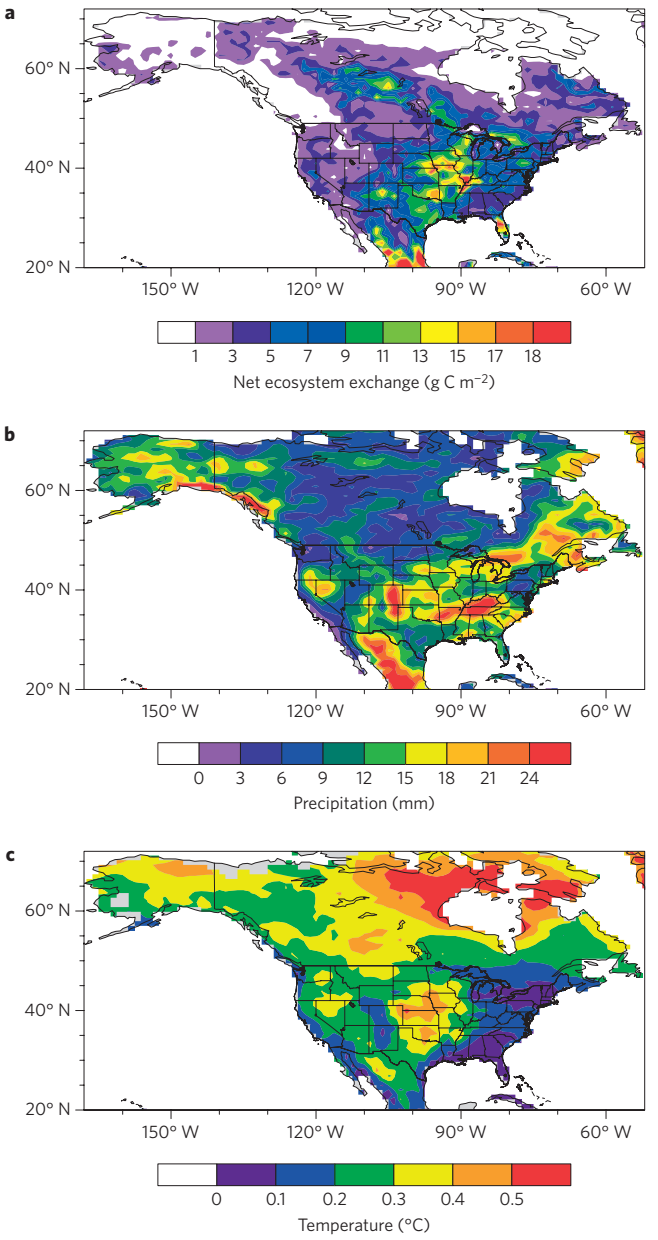

Figure 3 | Summertime ensemble variability in CCSM4. a, Standard deviation of the six-member CCSM4 ensemble for total summer (June–August) NEE at the end of the twenty-first century (averaged for the 20-year period 2080–2099). **b**, As in **a**, but for total summer precipitation. **c**, As in **a**, but for mean summer temperature.

Methods

The Community Climate System Model version 4 (CCSM4) consists of a finite volume nominal 1° (0.9° × 1.25°) 26-level implementation of the Community Atmosphere Model version 4 (CAM4) with coupled ocean, land and sea ice components. The land component, the Community Land Model version 4 (CLM4), includes a terrestrial carbon cycle[28]. A seven-member ensemble of CCSM4 simulations was performed for the twentieth century using historical forcings (1850–2005) and six simulations were extended through the twenty-first century for RCP8.5 (ref. 7). The RCP8.5 simulations, as well as other RCPs, were submitted for the Coupled Model Intercomparison Project phase 5 (CMIP5) experiments (publically available online at cmip-pcmdi.llnl.gov). These simulations used a prescribed trajectory of CO_2 concentration with concentrations specified by the CMIP5 protocol[29]. The terrestrial carbon cycle responds to that concentration, and the resulting changes in climate, but does not feedback to the atmospheric CO_2 concentration. These concentration-driven carbon-cycle simulations have been analysed as part of CMIP5 (refs 2,4).

All ensemble members were run with identical experimental conditions, but differed in initialization. The different initial conditions produced different climate trajectories, each of which is an equally likely realization. The different ensemble members provide an indication of climate variability within the model arising from random internal variation.

Net ecosystem exchange (NEE) aggregates ecosystem carbon sinks and sources into a total ecosystem carbon flux that determines whether the ecosystem is a net source (positive value) or sink (negative value) of carbon. Simulated net land–atmosphere exchange is the difference between carbon uptake during gross primary production (GPP), carbon loss during ecosystem respiration (ER), and non-respiratory carbon losses. Ecosystem respiration (ER) consists of autotrophic respiration from plants (Ra) and heterotrophic respiration from microbes (Rh), that is, ER = Ra + Rh. Net primary production is GPP − Ra.

To assess whether the magnitude of variability was similar in observed and simulated carbon fluxes, we compared observed NEE at the Harvard Forest eddy covariance flux tower with NEE for the comparable CCSM4 model grid cell. We used Harvard Forest flux data because it is one of the longest continuous time series of NEE, and because the NEE is well-documented[13]. The observations show increasing carbon uptake, and we assessed variability by taking the anomaly from the detrended time series.

We quantified ensemble variability as the standard deviation of the 20-year (2080–2099) mean total summer (June–August) NEE, temperature and precipitation across the six-ensemble members. To identify atmospheric variables causing the carbon-cycle variability, we correlated carbon flux anomalies with temperature and precipitation anomalies for the summer season (June–August average). Anomaly was defined as the deviation of an individual ensemble member from the ensemble mean. We examined the 20-year period 2080–2099 for each of the six ensemble members (a total of $n = 120$ data points) for each model grid cell. Both the standard deviations and the correlations vary geographically, and we illustrated them for North America during the summer season when metabolic activity (and consequently land carbon flux) was greatest, and therefore most strongly influenced by the physical environment.

The time of emergence is defined as the year at which the climate change signal (S) exceeds the noise (N) by a particular threshold[10]. Changes in carbon fluxes are nonlinear and are not monotonic, with periods of net carbon gain or loss over the years. We defined the signal as the ensemble mean change in ecosystem carbon, calculated as the sum of total vegetation carbon (CMIP5 variable 'cVeg') and total soil carbon (CMIP5 variable 'cSoil'), relative to year 2011. Change in ecosystem carbon integrates NEE over time, and is consequently less variable than NEE. We defined the noise as the standard deviation of the individual ensemble members.

We also analysed the signal-to-noise ratio in other CMIP5 model ensembles that included a carbon cycle in their RCP8.5 simulations. To be included in our analyses, we required the model to include four or more ensemble members, simulations to run for the entire twenty-first century, and the output to include total vegetation carbon and total soil carbon. Models meeting these requirements included a five-member ensemble of RCP8.5 simulations for CanESM2 ($2.8° \times 2.8°$) and a four-member ensemble for HadGEM2-ES ($1.24° \times 1.8°$). For CanESM2, the cumulative change in land carbon at the end of the twenty-first century, relative to 2005, is approximately 100 Pg C (ref. 2). The model ranks ninth for soil carbon and seventh for vegetation carbon skill among the CMIP5 models[9]. For HadGEM2-ES, the cumulative change in land carbon is approximately 350 Pg C (ref. 2), and the model ranks 6th for soil carbon and 11th for vegetation carbon skill[9].

Received 8 November 2013; accepted 1 July 2014; published online 27 July 2014

References

1. Friedlingstein, P. *et al.* Climate–carbon cycle feedback analysis: Results from the C4MIP model intercomparison. *J. Clim.* **19,** 3337–3353 (2006).
2. Jones, C. *et al.* Twenty-first-century compatible CO_2 emissions and airborne fraction simulated by CMIP5 Earth system models under four Representative Concentration Pathways. *J. Clim.* **26,** 4398–4413 (2013).
3. Arora, V. K. *et al.* Carbon-concentration and carbon–climate feedbacks in CMIP5 Earth system models. *J. Clim.* **26,** 5289–5314 (2013).
4. Friedlingstein, P. *et al.* Uncertainties in CMIP5 climate projections due to carbon cycle feedbacks. *J. Clim.* **27,** 511–526 (2014).
5. Meehl, G. A. *et al.* Combinations of natural and anthropogenic forcings in twentieth-century climate. *J. Clim.* **17,** 3721–3727 (2004).
6. Meehl, G. A. *et al.* Climate change projections for the twenty-first century and climate change commitment in the CCSM3. *J. Clim.* **19,** 2597–2616 (2006).
7. Meehl, G. A. *et al.* Climate system response to external forcings and climate change projections in CCSM4. *J. Clim.* **25,** 3661–3683 (2012).
8. Deser, C., Knutti, R., Solomon, S. & Phillips, A. S. Communication of the role of natural variability in future North American climate. *Nature Clim. Change* **2,** 775–779 (2012).
9. Anav, A. *et al.* Evaluating the land and ocean components of the global carbon cycle in the CMIP5 Earth system models. *J. Clim.* **26,** 6801–6843 (2013).
10. Hawkins, E. & Sutton, R. Time of emergence of climate signals. *Geophys. Res. Lett.* **39,** L01702 (2012).
11. Deser, C., Phillips, A., Bourdette, V. & Teng, H. Uncertainty in climate change projections: The role of internal variability. *Clim. Dyn.* **38,** 527–546 (2012).
12. Lawrence, P. J. *et al.* Simulating the biogeochemical and biogeophysical impacts of transient land cover change and wood harvest in the Community Climate System Model (CCSM4) from 1850 to 2100. *J. Clim.* **25,** 3071–3095 (2012).
13. Urbanski, S. *et al.* Factors controlling CO_2 exchange on timescales from hourly to decadal at Harvard Forest. *J. Geophys. Res.* **112,** G02020 (2007).
14. Keenan, T. F. *et al.* Terrestrial biosphere model performance for inter-annual variability of land–atmosphere CO_2 exchange. *Glob. Change Biol.* **18,** 1971–1987 (2012).
15. Mahlstein, I., Hegerl, G. & Solomon, S. Emerging local warming signals in observational data. *Geophys. Res. Lett.* **39,** L21711 (2012).
16. Thomas, R. Q., Zaehle, S., Templer, P. H. & Goodale, C. L. Global patterns of nitrogen limitation: Confronting two global biogeochemical models with observations. *Glob. Change Biol.* **19,** 2986–2998 (2013).
17. Richardson, A. D. *et al.* Environmental variation is directly responsible for short- but not long-term variation in forest–atmosphere carbon exchange. *Glob. Change Biol.* **13,** 788–803 (2007).
18. Chen, B. *et al.* Seasonal controls on interannual variability in carbon dioxide exchange of a near-end-of rotation Douglas-fir stand in the Pacific Northwest, 1997–2006. *Glob. Change Biol.* **15,** 1962–1981 (2009).
19. Dragoni, D. *et al.* Evidence of increased net ecosystem productivity associated with a longer vegetated season in a deciduous forest in south-central Indiana, USA. *Glob. Change Biol.* **17,** 886–897 (2011).
20. Nemani, R. R. *et al.* Climate-driven increases in global terrestrial net primary production from 1982 to 1999. *Science* **300,** 1560–1563 (2003).
21. Janssens, I. A. *et al.* Productivity overshadows temperature in determining soil and ecosystem respiration across European forests. *Glob. Change Biol.* **7,** 269–278 (2001).
22. Dunn, A. L. *et al.* A long-term record of carbon exchange in a boreal black spruce forest: Means, responses to interannual variability, and decadal trends. *Glob. Change Biol.* **13,** 577–590 (2007).
23. Piao, S. *et al.* Net carbon dioxide losses of northern ecosystems in response to autumn warming. *Nature* **451,** 49–52 (2008).
24. Pilegaard, K. *et al.* Increasing net CO_2 uptake by a Danish beech forest during the period from 1996 to 2009. *Agric. For. Meteorol.* **151,** 934–945 (2011).
25. Ballantyne, A. P., Alden, C. B., Miller, J. B., Tans, P. P. & White, J. W. C. Increase in observed net carbon dioxide uptake by land and oceans during the past 50 years. *Nature* **488,** 70–72 (2012).
26. Stott, P. A. *et al.* Detection and attribution of climate change: A regional perspective. *WIREs Clim. Change* **1,** 192–211 (2010).
27. Meehl, G. A. *et al.* Decadal prediction: Can it be skillful? *Bull. Am. Meteorol. Soc.* **90,** 1467–1485 (2009).
28. Lawrence, D. M. *et al.* Parameterization improvements and functional and structural advances in version 4 of the Community Land Model. *J. Adv. Model. Earth Syst.* **3,** M03001 (2011).
29. Taylor, K. E., Stouffer, R. J. & Meehl, G. A. An overview of CMIP5 and the experiment design. *Bull. Am. Meteorol. Soc.* **93,** 485–498 (2012).

Acknowledgements

We would like to thank C. Deser and B. Stephens for helpful feedback that redefined our initial analyses. We would also like to thank the reviewers for the constructive comments that have improved the final version of this paper. The National Center for Atmospheric Research is sponsored by the National Science Foundation. This work was supported by National Science Foundation grant EF-1048481.

Author contributions

G.B.B. and D.L. conceived the project. D.L. assembled model datasets and analysed the simulations, with guidance from G.B.B. and D.W.N. All authors contributed to writing the paper.

Additional information

Supplementary information is available in the online version of the paper. Reprints and permissions information is available online at www.nature.com/reprints. Correspondence and requests for materials should be addressed to D.L.

Competing financial interests

The authors declare no competing financial interests.